External magnetic field effect on plume images and X-ray emission from a nanosecond laser produced plasma

M.S. RAFIQUE, M. KHALEEQ-UR-RAHMAN, I. RIAZ, R. JALIL, AND N. FARID

Department of Physics, University of Engineering and Technology, Lahore, Pakistan

Abstract

The plume images of the laser produced silver plasma in the absence and presence of 0.45 T transverse magnetic field has been investigated under vacuum $\sim 10^{-4}$ torr and in air. An Nd:YAG laser (1.064 μm, 1.1 MW, 9 ns) with intensity $\sim 10^{12}$ Wcm^{-2} was used to generate plasma. A CCD image capture system was used for plasma imaging to explore the plume. A magnetic probe was employed to measure the variation in internal magnetic field of plasma with as well as without 0.45 T external transverse magnetic field. The X-ray emission from plasma in both the cases (with and without B field) was also monitored using two PIN photodiodes filtered with 24 μm Cu and 24 μm Al. The plume images in both the cases were then correlated with the time resolved soft X-ray emission. It was found that the self generated magnetic field of the plasma increases in the presence of magnetic field. Plume images reveal that the confinement of the plume takes place in the presence of magnetic field both in the cases of air and vacuum. Jet and spikes like structures were also observed due to plasma instabilities. Lobe formation in the plume at latter stages of plasma evolution was more prominent in air than under vacuum. X-ray emission signals exhibited an enhancement in the emission under transverse magnetic field. An increased rate of recombination due to high density as a result of plasma confinement across the applied magnetic field was found to be the main reason behind emission enhancement.

Keywords: CCD; LPP; Nd:YAG laser; PIN photodiodes; Soft X-rays

INTRODUCTION

In recent years, the use of magnetic field to confine laser-induced plasmas has attracted more and more interest. The magnetic field can be employed to better control the dynamic properties of the transient and energetic plasmas. The presence of a magnetic field during the expansion of laser-induced plasmas may initiate several interesting phenomena, including conversion of the plasma kinetic energy, plume confinement, ion acceleration, X-ray emission enhancement, plasma instabil-ities, etc. The control of plasma properties have various research applications such as beam heating of magnetically confined thermonuclear plasma during the inertial confinement fusion (ICF) (Shen *et al.*, 2006; Hora, 2007; Anwar *et al.*, 2006). The presence of external magnetic field (Virendra *et al.*, 2003; Pisarczyk *et al.*, 2000; Torrisi *et al.*, 2007) can be used to control the velocity of high energy particles before they implant during ICF (Harilal *et al.*, 2004). Collimation and stability properties (Harilal *et al.*, 2004) are easily controllable by the applied external magnetic field to the laser induced plasma. It is helpful in the mitigation of the debris including energetic ions, vapors, particulates, and molten globules from the laser plasma in lithography (Rai *et al.*, 2000; Harilal *et al.*, 2005; Sizyuk *et al.*, 2007; Ozaki *et al.*, 2007). It reduces the number of large plasma species during thin films growth by pulse laser deposition (PLD) with the magnetic force applied on plasma particulates (Jordan *et al.*, 1997; Tsui *et al.*, 2002). The study of laser plasma evolution under magnetic field is helpful to understand the physical phenomena such as bipolar flow associated with young stellar objects, interaction of solar wind with planetary magnetosphere, formation of jets (Kaspeczuk *et al.*, 2007; Schaumann *et al.*, 2005), propulsion of space vehicles (Deutsch & Tahir, 2006), and working of magneto hydrodyn-amic generator (Harilal *et al.*, 2004; Shen *et al.*, 2006; Pant *et al.*, 1998).

The understanding of plasma dynamics including con-version of thermal energy into kinetic energy, ion accelera-tion, instability (Shen *et al.*, 2006; Harilal *et al.*, 2006; Pant *et al.*, 1998), and the emission of radiation from the laser produce plasma (Neogi & Theraja, 1999; Virendra *et al.*,

Address correspondence and reprint request to: M. Shadid Rafique, Department of Physics, University of Engineering and Technology, Lahore. E-mail: pakistanshahidrafiq@uet.edu.pk

2003) in an external magnetic field is very useful. It has been reported that the laser plasma in magnetic field alters the plasma dynamics, which results in the variation of density, velocity and temperature of plasma particles, and the radiation emission from plasma is also enhanced (Harilal *et al.*, 2004, 2006; Shen *et al.*, 2006; Kumar, 2003). The soft X-rays emitted from the laser plasma have variety of applications in various fields (Fang & Ahmad, 2007; Schade *et al.*, 2006). Investigations on the interaction of soft X-rays intensities bellow ablation threshold with solid surfaces have attracted many researchers. The X-ray intensities are capable of controlled machining of the materials to make surface smooth at nano-meter scale (Makimura *et al.*, 2006). In addition, applying the interaction, one could expect direct photo-nano-machining of materials at a precision as high as the diffraction limit of the soft X-rays (Makimura *et al.*, 2005).

X-rays from the laser plasma have been utilized to study the optical luminescence and low-dimenionality photo-luminescent patterns from complex materials (Kim *et al.*, 2003; Baldacchini *et al.*, 2002) and to explore their stability. The instability or decomposition has been exploited to write microscopic metal lines and create light storage devices. The X-ray induced decomposition of nitride containing materials indicates that X-ray may be used to directly write patterns on the surface (Butenko *et al.*, 2006). Soft X-ray irradiation affects the chemical and physical properties of semi-fluorinated mono-layered materials (Wagner *et al.*, 2002). X-ray irradiated polymers exhibit modification in the complex refractive index within the irradiated volume, which is a critical parameter deriving the behavior of the material as a light waveguide (Montereali *et al.*, 2007).

Besides the spectroscopic application, soft X-rays are found to have strong impact on the characteristics of the diamond devices used for the radiation detection resulting in improved charge collection efficiency (Hordiquin *et al.*, 2001). A variety of techniques are in use to optimize the parameters of the plume as well as the X-rays generated from the laser plasma for their applications at the best precision level (Shaihd Rafique *et al.*, 2005). One of the techniques is to apply the external magnetic filed to the plasma produced by laser to better control the governing parameters, like density, confinement, length of the plume, X-ray emission intensities, etc.

This paper represents the effect of applied external magnetic field on the self generated magnetic field of the plasma, evolution of plume, and the soft X-ray emission in air and vacuum. For this purpose, a steady transverse magnetic field of 0.45 T is applied to plasma plume induced from silver target by an Nd:YAG laser of intensity $\sim 10^{12}$ W/cm^2. The plume evolution is also correlated with the X-ray emission from the plasma under vacuum $\sim 10^{-4}$ torr as well as in air. The X-ray emission is enhanced after the application of the external magnetic field regardless of the environment (air or vacuum). The results can be helpful in the guiding of plasma by magnetic field for a uniform film growth by pulsed laser

deposition. The magnetic field applied to laser produced plasma can be helpful in getting debris free plasma source for X-rays lithography. The enhanced X-ray emission from laser produced plasma (LPP) can be a better tool in laser induced breakdown spectroscopy (LIBS), optical luminescence spectroscopy (OLS), nano machining, etc.

EXPERIMENTAL SETUP

A passive Q-switched Nd:YAG laser of 10 mJ energy and 10^{12} W/cm^2 intensity with pulse duration of 9–14 ns was used to produce Ag plasma. The laser was focused on the target by an infrared transmitting lens of 10 cm focal length. Helmholtz coils providing a steady magnetic field of 0.45 T were used as a source of external magnetic field applied perpendicular to the plume propagation direction. The experiments were carried out under vacuum $\sim 10^{-4}$ torr as well as in air.

To diagnose the self generated magnetic field of the plasma, a magnetic probe with proper biasing was employed. The probe was placed inside the vacuum chamber at a distance of 2 mm from the target with the magnetic probe's tip making an angle 45° with the target surface.

Two PIN photodiodes, one filtered with 24 μm Cu, and second with 24 μm Al were used to investigate the time-resolved X-ray emission from LPP in the presence and absence of externally applied magnetic field. These filters were chosen because of their peak response (1eV to 4 KeV) in the soft X-rays region (Rafique, 2000). A CCD based image capture system was employed for the imaging of the plasma plume. The signals from PIN photodiodes and magnetic probe were recorded on a 4-channel 500 MHz YOKOGAWA digital storage oscilloscope. A schematic of the experimental setup (a) along with the magnetic probe arrangement (b) is shown in Figure 1.
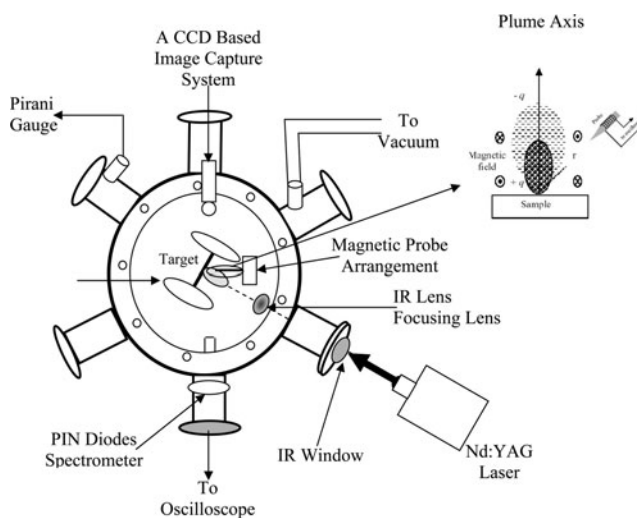

Fig. 1. (**a**) A schematic arrangement of experimental setup. (**b**) A schematic of the magnetic probe arrangement.

RESULTS AND DISCUSSION

Ablation of the silver under vacuum creates an intense luminous plume that expands normal to target surface. The plasma has an elliptical shape with contours along the propagation direction. The initial density gradients and pressure inside plume result in plasma in the direction perpendicular to the target surface than in the lateral direction. The induced voltage is developed due to the time varying magnetic field during the evolution and intense bursts of soft X-rays are also emitted.

Magnetic Probe, PIN Diode Signal Profiles, and Plume Images (with B = 0 and B = 0.45T) Under Vacuum

Figure 2 shows the time resolved magnetic probe signal with a peak of 160 mV recorded on the oscilloscope (channel 1) under vacuum without external magnetic field i.e., (B = 0). This magnetic probe signal has two consecutive positive peaks and a negative peak of large amplitude. First positive peak is due to the magnetic field generated by the electrons. As soon as the plasma plume is formed, the generated electrons propagating in the direction perpendicular to the target surface come into the region of magnetic probe earlier, and varying magnetic field generated by motion of these electrons induces the varying electric field whose potential is taken on the output. The electrons due to high

Fig. 2. Laser induced silver plasma under vacuum with B = 0 T. (**a**) Signal profiles of Magnetic probe (channel I), PIN diode with 24 μm Cu filtre (channel II), and with 24 μm Al filtre (channel III). (**b**) CCD image of the plume.

diffusivity come out from the vicinity of the magnetic probe after giving a peak for a few ns. The peak goes to zero as the electrons go out of the region of the magnetic probe. The ions due to their less mobility are far behind the electrons inside the plasma. A strong electric field is developed which attracts the forward moving electrons backward. These electrons during their backward motion again come into the magnetic probe region and magnetic probe becomes active giving a positive peak due to the varying magnetic field of the returning electrons in plasma. A negative peak is observed indicating the voltage developed by the ions. At this stage the slow moving ions of plasma have reached the probe region and their varying magnetic field induces the potential in the magnetic probe coil.

X-ray signal profile from PIN photodiodes (Fig. 2, channel II and III) has exactly the same time resolved behavior but with difference in the time duration of their production. The signal at channel II (Cu filter) with peak at 60 mV lasts for about 40 ns and the signal at channel III (Al) filter with peak at 25 mV lasts for less than 40 ns.

As far as the image of the plasma under vacuum is concerned (Fig. 2b), the plume evolutes perpendicular to the target in a normal way without known flute instabilities. At the final stage a nipple seems to appear at the front of the plume, which might be due to the ambient recoil pressure.

When the plasma is placed across the transverse magnetic field of 0.45 T, it radically altered the properties of plasma due to the fact that the motion of changed particles is affected by the applied magnetic field. In the presence of external magnetic field, the electron and the ions cannot move freely in the direction perpendicular to the lines of forces. The trajectory of particles now becomes helical with axis in the direction of the magnetic field. The behavior of the plume is not much affected at early stage but it is slowed down considerably with time.

Figure 3a shows the signal profiles of magnetic probe (channel I), X-ray (channel II and channel III), and CCD images (Fig. 3b) of the plasma in the presence of the 0.45 T magnetic field. The overall magnetic probe signal with the peak of 180 mV, which lasts for about 50 ns. The internal self generated magnetic field of electrons increases from 45 mT (B = 0) to 65 mT. This increase in internal magnetic field is attributed to the rapid charges in electric field of plasma. The larmour radius of the plasma species increases under the influence of the transverse magnetic field. The ions experience an upward magnetic force whereas the electron will experience a downward magnetic force of equal magnitude by the applied magnetic field. There is also an increase in the time direction of first and second peaks of the electron signal in the presence of transverse magnetic field. The signal time rises from 40 ns (B = 0) to 50 ns. The broadening of time scale in the presence of field is the results of enhanced collisionality which in turn slows down the plasma species.

The applied uniform transverse magnetic field results in the decrease of electron loss by the diffusion. As a result of
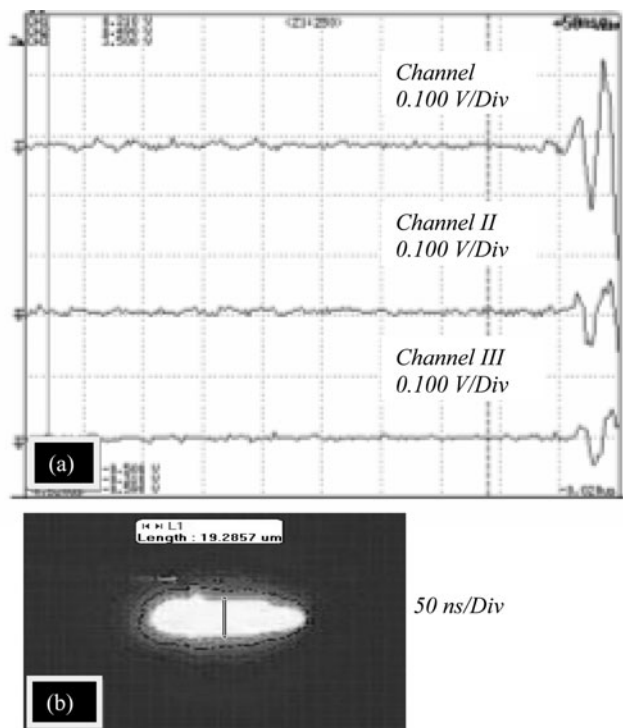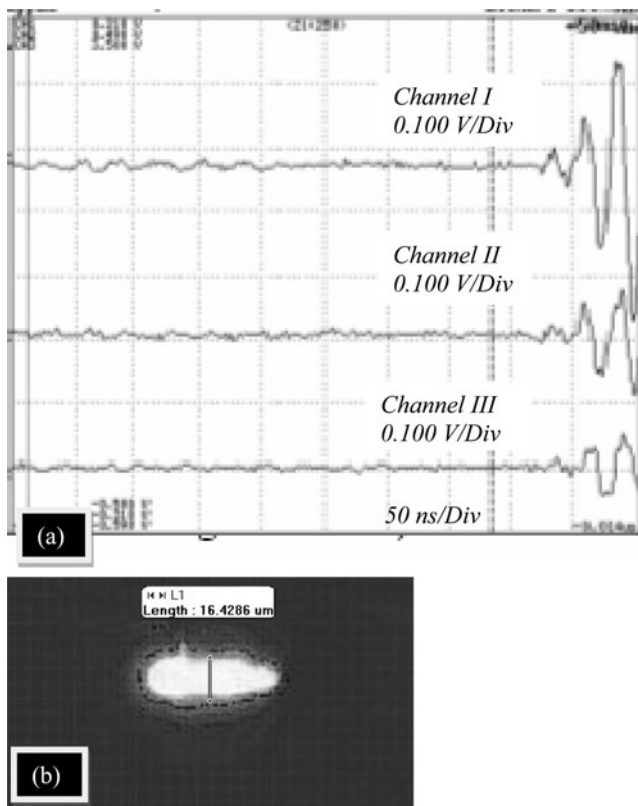
Fig. 3. Laser induced silver plasma under vacuum with B = 0.45 T. (**a**) Signal profiles of Magnetic probe (channel I), PIN diode with 24 μm Cu filtre (channel II), and with 24 μm Al filtre (channel III). (**b**) CCD image of the plume.

which the time duration for stay of electrons in the magnetic probe region increases. After the formation of LPP the temperature, density and thermal pressure (nkT_e) of plasma are high, and as the plasma expands the temperature and the density of plasma plume decreases resulting in low plasma pressure (Pant *et al.*, 1998; Neogi & Theraja, 1999) due to angular distribution (Rafique, 2005; Farynski *et al.*, 1992) of the plasma species. Due to plasma confinement across magnetic field there is an increase in collision of plasma species and they are slowed down (Harilal *et al.*, 2004; Rai *et al.*, 2000).

Time profile study of plasma plume shows that in the presence of magnetic field the lifetime of plasma plume increases. The magnetic force of the applied magnetic field results in the confinement which increases the plasma constituents in the confinement region (Jordan *et al.*, 1997). Due to instabilities (Shen *et al.*, 2006) at the boundary of plasma or due to diffusion process there is loss of plasma species from confinement region. The signal profiles of X-rays (channels II and III, Fig. 3a) exhibit an increase in the emission as indicated by the peaks of the signals. The signal from the PIN diode filtered with Cu has a maximum at 90 mV while PIN diode filtered with Al has a peak of 35 mV. In comparison to the X-ray signal profiles

an increase in the emission is observed under the influence of B = 0.45 T field which shows that the emission has been increased collectively by the bremsstrahlung, line radiation and recombination across the magnetic field. Emission from the plasma mainly depends on the plasma β, which is a function of the plasma density, temperature, and external magnetic field. The main reason behind the enhancement in emission is an increase in rate of recombination of ion and electrons in plasma due to high density (due to confinement). Basically, increase in X-ray emission signal is expected because of the increase in plasma density as a result of the decrease in plasma velocity in the axial direction due to the transverse magnetic field. X-ray intensity due to Bremsstrahlung, recombination, or line radiation are all directly proportional to the square of the plasma density. The enhancement in the X-ray emission is in agreement with the previously reported work (Harilal *et al.*, 2004, 2006; Shen *et al.*, 2006).

The image of the plume under the influence of external magnetic field is shown in Figure 3b. In the presence of transverse magnetic field plume propagation is considerably slowed down and confined in a direction perpendicular to the target surface i.e., in the axial direction of plasma plume. The effect of external magnetic field interaction mainly depends on the properties of the outer layer of the plume, which shields the interior of plasma from the magnetic field. Plasma expansion across transverse magnetic field occurs in both diamagnetic and non-diamagnetic limits.

Plasma particle pressure/magnetic pressure (β) is an important dimensionless quantity as far as the effect of magnetic field on plasma is concerned. Initially, as the plasma plume is formed, the particle pressure is very high due to high value of pressure and density. The value of β is on the order of a few thousand indicating that plume is in the diamagnetic limits. When an external magnetic field is applied, the electrons and ions in the plasma are influenced by the Lorentz force, and the expansion and diffusion of plasmas are decelerated by the magnetic field. From maneto-hydrodynamical (MHD) equation, the parameter β of plasma is given by (Shen *et al.*, 2006).

$$\beta \equiv \frac{8\pi nkT_e}{B^2}. \tag{1}$$

The parameter β indicates the size of the diamagnetic effect. The deceleration of the plasma expansion under the influence of magnetic field can be given as

$$\frac{v_2}{v_1} = \left(1 - \frac{1}{\beta}\right)^2. \tag{2}$$

Where v_1 and v_2 are, respectively, the asymptotic plasma expansion velocity in the absence and in the presence of the magnetic field. When $\beta = 1$, the plasma would be stopped by the magnetic field. In the case of high β, the magnetic confinement would not be obvious. In the case of low β

plasma, as in our case, it is 9.16×10^{-3}, the magnetic confinement would be effective.

Diamagnetic currents in the outer layer of plasma exclude the magnetic field from interior of the plume and may interact with the uniform external magnetic field of 0.45 T and expansion continues as a result of larger β until the kinetic pressure becomes greater than the magnetic pressure. But as the plasma expands the density and pressure decreases and hence the resistance offered by external applied magnetic increases resulting in the decrease value of "β." Plasma plume will now become in non-diamagnetic limit and the applied magnetic field diffuses into plasma. In this way, the laser produced plasma diamagnetic cavity expands until the total excluded magnetic energy becomes comparable to the plasma energy. The expansion of plume stops when magnetic pressure is balanced by plasma pressure or $\beta = 1$. At this stage, plasma confinement and stagnation take place when the kinetic pressure becomes equal to the plasma pressure. It has been postulated that a cloud of laser produced plasma will be stopped by a magnetic field B in a distance $R_b \sim B^{-2/3}$ (Shen *et al.*, 2006), where R_b is the confinement radius. Before the plasma reaches R_b, the leading edge developed distinct flute structures or spikes that projected out from the plasma (as can be seen in Fig. 3b).

Perfect confinement is possible only when plasma is fully conducting, which is not possible for present experimental conditions, and a part of the plasma will erase ions from the confinement region due to cross-field diffusion as a result of the increased collision or due to generation of instability in plasma.

The density fluctuations in plasma can also occur due to the oscillation of magnetic field lines under the effect of the plasma pressure and restoring force due to the magnetic field lines. Instabilities are also observed due to plasma oscillations in magnetic field. The jet like instability takes place in the plane of the transverse magnetic field. The slowing down of plasma species or enhanced collisionality both results in the decrease in the diffusion of the plasma species especially electrons which lead to the increased time duration of the signals of magnetic probe.

Magnetic Probe, PIN Diode Signal Profiles and Plume Images (with B = 0 and B = 0.45 T) in Air

The variation in the plasma B field, X-ray emission, and plasma images of a silver plasma were also explored in air without and with the application of a transverse magnetic field of strength 0.45 T. When the laser falls on the silver surface, the thermal energy is converted into kinetic energy of ions, and the electron density is observed to decay exponentially. Channel I in Figure 4 is the magnetic probe signal of silver plasma in air. The signal has two positive peaks generated by electrons. The magnetic probe signal with peak voltage of 70 mV lasts for 45 ns. The signal carries two peaks. The first peak of electrons shows that the time varying magnetic field of the electrons inside the
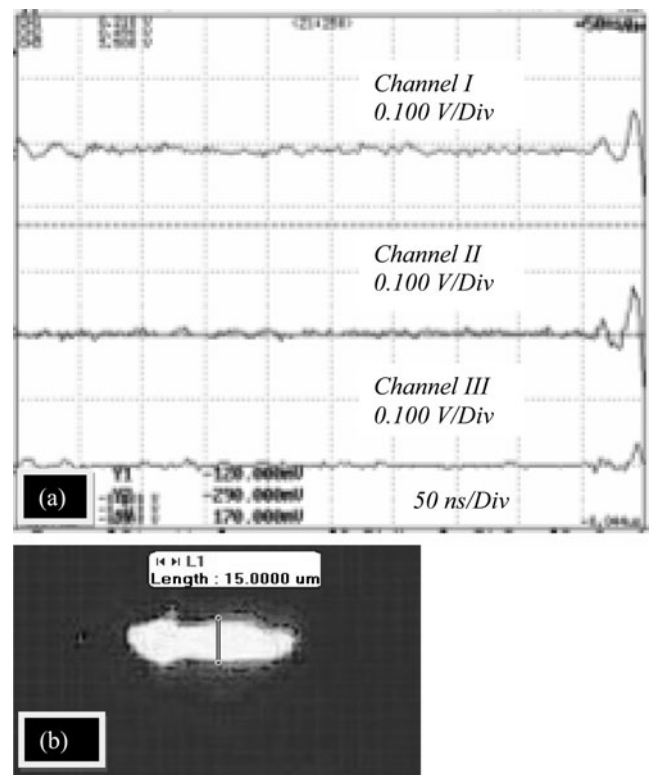

Fig. 4. Laser induced silver plasma in air with B = 0 T. (**a**) Signal profiles of magnetic probe (channel I), PIN diode with 24 μm Cu filtre (channel II) and with 24 μm Al filtre (channel III). (**b**) CCD image of the plume.

plasma induces voltages. The electrons being lighter and more mobile than ions come into the probe region earlier giving their first peak. These electrons also have high diffusivity so they came out of the probe regions. The outgoing electrons experience strong electric field produced by the separation between the slow moving heavy ions and the forward moving electrons. As a result of this electric force, the electrons are attracted backward, and in their returning state they again come into the probe region giving rise to a second peak. The X-ray signals profiles from two filtered (Cu and Al) PIN photodiodes in Figure 4 (channel II and channel III) are produced due to combined result of the bremsstrahlung, recombination and line radiations.

The X-ray signal (channel II) carries a peak of 60 mV lasting for 40 ns. The signal exhibit two time resolved peaks. The first X-ray peak arises as a result of the X-ray generation due to the interaction of free electrons at the surface of the silver target when laser impinges on the target surface, and the second peak of the X-ray signal is attributed to the X-rays emission as a result of the Bremsstrahlung, recombination, and line radiation during backward motion of electron by the electric field pull between fast moving electrons and relative by slow moving ions. The second PIN photodiode (channel III) produces an X-ray signal of 29 mV which stays for 15 ns (major peak). The plume image in air (Fig. 4b) with B = 0 seems to have a normal texture with
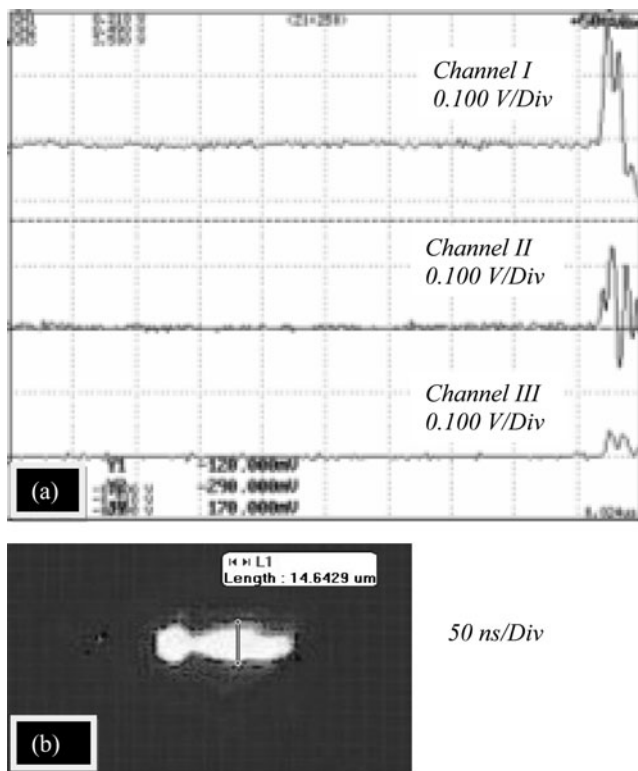
Fig. 5. Laser induced silver plasma in air with B = 0.45 T. (**a**) Signal profiles of magnetic probe (channel I), PIN diode with 24 μm Cu filtre (channel II) and with 24 μm Al filtre (channel III). (**b**) CCD image of the plume.

limit due to plasma cooling, the magnetic field is able to diffuse across the plasma plume boundary.

The transverse magnetic field of 0.45 T applies a magnetic force on the plasma species which results in an increase of the larmour radius of these ions and electrons, and their varying electric field produces varying magnetic field giving a voltage signal of 190 mV, which stays for 34 ns. In the presence of the transverse magnetic field, the plume propagation is slowed down and confined in a direction perpendicular to the target surface. The slowing down of the plasma species is attributed to the MHD model in which the kinetic energy of expansion is converted into electron motion. There is an increase in the time duration of the electron signal up to 34 ns, which indicates that the electrons stays more in the probe region. This is due to slowing down of electrons in the presence of magnetic field. The loss of the electron from the magnetic probe region due to high diffusivity has been decreased.

The jet like spikes in the output signal of the magnetic probe is due to the instabilities produced as a result of the pressure gradients inside the plasma plume (as can be seen in the plume image Fig. 5b). The pressure gradients give rise to the oscillations resulting in plasma instabilities. The absence of the ion signals in air indicates that the presence of the different elements in air has slowed down the silver plasma ions. The signal profile of magnetic probe in air indicates the absence of the negative peak which is due to the magnetic field of the ions. The absence of magnetic field signals of ions depicts that when the plasma is produced in air, the impurities or constituents of air play their role and hinders the ions motion by ion absorption, scattering, or reflection. As a result, the ions have not reached the magnetic probe region.

Two PIN photodiodes (channels II and III) detected the X-ray emission from silver plasma placed in a transverse magnetic field. An increase in the X-ray emission is clearly observed. The increase is attributed to the collective increase in X-ray emission by bremsstrahlung, recombination, and line radiation.

The first PIN photodiode at channel II (Fig. 5a) gives a peak voltage of 130 mV with time duration of 38 ns. The second PIN photodiode at channel III (Fig. 5a) gives X-ray emission for 25 ns with a peak voltage of 40 mV. The confinement of the silver plasma with the transverse magnetic field has increased the density of the plasma. This result in the enhanced rate of recombination and also other processes of X-ray emission as Bremsstrahlung and line radiation contribute more actively.

The distortion in the X-ray emission signals of PIN photodiodes in air is due to contribution of other air composite particles. The signal of X-ray emission fluctuation is due to variation in the X-ray emission and intensity.

Figure 5b shows the plume image expansion under the influence of 0.45 T filed. The plume looks like a jet. The induced currents are caused by the interaction of the field with plasma and hence the plasma will leak out laterally resulting in the jet formation as observed in plume images.

no other significant appearance. However, the expansion of the plume in the axial direction (normal to the target surface) is a bit less than that in vacuum; the reason is obviously the ambient air pressure restricting the plume evolution. Also, at the trailing edge, there appears an onset of instability trying to compress the plume. The behavior of the silver plasma is drastically altered when the expansion takes place in air under the effect of the 0.45 T transverse magnetic field. Figure 5a shows the signal profiles of magnetic probe (channel I), two filtered PIN diodes (Cu filter channel II and Al filter channel III).

The magnetic probe shows a changed behavior. The change in the magnetic probe signal is due to the interaction of plasma species with the different elements of air and influence of magnetic field on plasma particles. As the plasma expansion proceeds, the density and temperature falls rapidly. One of the most important parameter for the expansion into a magnetic field is the plasma β. Initially, after the conversion of thermal energy into kinetic energy, the β has significantly higher values, and plasma is in the regime of diamagnetic expansion. Diamagnetic currents exclude the external magnetic field from the interior of plasma and may interact with the uniform magnetic field through $\mathbf{J} \times \mathbf{B}$ force. The acceleration and deceleration depends on the direction of the diamagnetic currents. In the latter phase of plume expansion, the plasma is in the non-diamagnetic

There is a compressed portion of the plume near the trailing edge indicative of the onset of instability. The instability might grow due to the interaction of the self generated plasma B field and the applied B field leading toward a resulting magnetic field compressing the plume. There is an overall confinement in the plume both in the axial and radial direction which might be due to the applied filed in conjunction with the ambient air pressure gradients.

Plasma evolution in the presence of applied magnetic field is not stable. As a result of interaction between magnetic field lines and energetic plasma at boundary various instabilities appear as structure like jets, flute, spikes, and spirals (Harilal *et al.*, 2004). One reason of these instabilities is density fluctuations produced due to oscillation of magnetic field lines under plasma and restoring force of magnetic field lines.

CONCLUSIONS

The magnetic behavior, X-ray emission, and plume imaging of silver plasma produced by 1.064 µm pulses of Nd:YAG laser in the absence and presence of 0.45 T transverse magnetic field have been investigated. The experiments were carried out both in air as well as under vacuum. It is concluded that self generated magnetic field of plasma species increases in the presence of transverse magnetic field regardless of the environment (vacuum or air) due to the magnetic force on plasma species, which results in increased electric field variation and ultimately enhancing the self generated magnetic field signal.

The X-ray emission from laser induced plasma expanding across a uniform transverse magnetic field both in air and under vacuum is enhanced. The collective effects in plume imaging as it is confined across the transverse magnetic field leads toward the enhanced collisionality, which causes the slowing of plasma species. The loss of electron from plasma confinement region due to various diffusion processes is controlled and this is supported by the time profile of magnetic probe signal, which is broadened in the presence of magnetic field. The plume appears more confined with the growth of instability in case of air as compared to that in vacuum. The magnetic field can be used to effectively control the confinement and enhance the emission of X-rays.

REFERENCES

Anwar, M.S., Latif, A., Iqbal, M., Rafique, M., Skhaleeq-Ur-Rahman, M. & Siddique, S. (2006). Theoretical model for heat conduction in metals during interaction with ultra short laser pulse. *Laser Part. Beams* 24, 347–353.

Baldacchini, G., Bongfigli, F., Flora, F., Montreali, R.M. & Murra, D. (2002). High contrast photoluinescent patterns in LiF crystals produced by soft X-rays from laser-plasma source. *Appl. Phys. Lett.*, 80, 4810.

Bashir, S., Rafique, M.S. & Ul-Haq, F. (2007). Laser ablation of ion irradiated CR-39. *Laser and Particle Beams*, 25, 181–191.

Butenko, Y.V., Alves, L., Brieva, A.C., Yang, J., Krishnamurthy, S. & Siller, L. (2006). X-ray induced decomposition of gold nitride. *Chem. Phys. Lett.* 430, 89.

Deutsch, C. & Tahir, N.A. (2006). Fusion reactions and matter-antimatter annihilation for space propulsion. *Laser Part. Beams* 24, 605–616.

Fang, X. & Ahmad, S.R. (2007). Saturation effect at high laser pulse energies in laser-induced breakdown spectroscopy for elemental analysis in water. *Laser Part. Beams* 25, 613–620.

Farynski, A., Gogolewski, P., Karpinski, L., Kusnierz, M., Makowski, J., Mroczkowski, M., Szczurek, M., Bryunetkin, B.A., Faenov, A.J. & Skobelev, I.J. (1992). Inverse population of the H-like f ion levels in a recombining laser-produced plasma confined in a strong magnetic-field. *Laser Part. Beams* 10, 801–809.

Harilal, S.S., O'Shay, B. & Tillack, M.S. (2005). Spectroscopic characterization of laser-induced tin plasma, *J. Appl. Phys.* 98, 13306.

Harilal, S.S., Tillack, M.S., O'Shay, B., Bindhu, C. & Najamabadi, V.F. (2004). Confinement and dynamics of laser-produced plasma expanding across a transverse magnetic field. *Phys. Rev. E* 69, 026413–1.

Harilal, S.S., Tillack, M.S., Tao, Y., O'Shay, B., Paguio, R. & Nikroo, A. (2006). Extreme-ultraviolet spectral purity and magnetic ion debris mitigation by use of low-density tin targets. *Opt. Lett.* 31, 1549.

Hora, H. (2007). New aspects for fusion energy using inertial confinement. *Laser Part. Beams* 25, 37–45.

Hordiquin, C., Tromson, D., Brambilla, A., Bergonzo, P. & Foulon, F. (2001). Strong impact X-ray radiation associated with e-beam metallization of diamond devices, *J. Appl. Phys.* 90, 2533.

Jordan, R., Cole, D. & Lunney, J.G. (1997). Pulsed laser deposition of particulate-free thin films using a curved magnetic filter. *Appl. Surf. Sci.* 109, 403.

Kasperczuk, A., Pisarczyk, T., Borodziuk, S., Ullschmied, J., Krousky, E., Masek, K., Pfeifer, M., Rohlena, K., Skala, J. & Pisarczyk, P. (2007). Interferometric investigations of influence of target irradiation on the parameters of laser-produced plasma jets. *Laser Part. Beams* 25, 425–433.

Kim, P.G., Brandys, M.C., Hu, Y., Puddephatt, R.J. & Sham, T.K.J. (2003). Soft X-ray excited optical luminesencs studies of gold (I) complex. *J. Lumin.* 105, 21.

Kumar, A. (2003). Effect of steady magnetic field on laser-induced breakdown spectroscopy. *Appl. Opt.* 42, 3662.

Makrimura, T., Miyomoto, Uchida, H.S., Fujimori, T., Niino, H. & Murakami, K. (2006). Nano ablation of inorganic materials using laser plasma soft X-rays at around 10 nm. *Jap. J. Appl. Phys.* 45, 5545.

Makrimura, T., Kenmotsu, Y., Miyamoto, H., Hiino, H. & Murakami, K. (2005). Ablation of silica glass using pulsed laser plasma soft X-rays. *Surf. Sci.* 593, 248.

Montereali, R.M., Bongfigli, F., Gregoratti, L., Kiskinova, M., Larciprete, R., Montecchi, M. & Nichelatti, E. (2007). Advanced optical characterization of active microstrips induced on LiF crystal by a monochromatic soft X-ray beam. *J. Non-Crystl. Solids* 353, 456.

NEOGI, A. & THERAJA, R.K. (1999). Dynamics of laser produced carbon plasma expanding in a nonuniform magnetic field. *J. Appl. Phys.* **85**, 1131.

OZAKI, T., BOM, L.B.E., GANEEV, R., KIEFFER, J.C., SUZUKI, M. & KURODA, H. (2007). Intense harmonic generation from silver ablation. *Laser Part. Beams* **25**, 321–325.

PANT, H.C., RAI, V.N. & SHUKLA, M. (1998). Behavior of expanding laser produced plasma in a magnetic field. *Phys. Scripta* **T75**, 104.

PISARCZYK, T., FARYNSKI, A., FIEDOROWICZ, H., GOGOLEWSKI, P., KUSNIERZ, M., MAKOWSKI, J., MIKLASZEWSKI, R., MROCZKOWSKI, M., PARYS, P. & SZCZUREK, M. (1992). Formation of an elongated plasma-column by a magnetic confinement of a laser-produced plasma. *Laser Part. Beams* **10**, 767–776.

RAFIQUE, M.S. (2000). Ph.D Thesis, Singapore: Nanyang Technological University.

RAI, V.N., SHUKLA, M. & PANT, H.C. (2000). Density oscillations in laser produced plasma decelerated by external magnetic field. *Pramana J. Phys.* **55**, 773.

SCHADE, W., BOHLING, C., HOHMANN, K. & SCHEEL, D. (2006). Laser-induced plasma spectroscopy for mine detection and verification. *Laser Part. Beams* **24**, 241–247.

SCHAUMANN, G., SCHOLLMEIER, M.S., RODRIGUEZ-PRIETO, G., BLAZEVIC, A., BRAMBRINK, E., GEISSEL, M., KOROSTIY, S., PIRZADEH, P., ROTH, M., ROSMEJ, F.B., FAENOV, A.Y., PIKUZ, T.A., TSIGUTKIN, K., MARON, Y., TAHIR, N.A. & HOFFMANN, D.H.H. (2005). High energy heavy ion jets emerging from laser plasma generated by long pulse laser beams from the NHELIX laser system at GSI. *Laser Part. Beams* **23**, 503–512.

SHAIHD RAFIQUE, M., KHALEEQ-UR-RAHMAN, M., ANWAR, M.S., MUHAMOOD, F., ASHFAQ, A. & SIRAJ, K. (2005). Angular distribution and forward peeking of laser produced plasma ions. *Laser Part. Beams* **23**, 131.

SHEN, X.K., LU, Y.F., GEBRE, T., LING, H. & HAN, Y.X. (2006). Optical emission in magnetically confined laser-induced breakdown spectroscopy. *J. Appl. Phys.* **100**, 053303-1.

SIZYUK, V., HASSANEIN, A. & SIZYUK, T. (2007). Hollow laser self-confined plasma for extreme ultraviolet lithography and other applications. *Laser Part. Beams* **25**, 143–154.

THAREJA, R.K. & SHARMA, A.K. (2006). Reactive pulsed laser ablation: Plasma studies. *Laser Part. Beams* **24**, 311–320.

TORRISI, M.L.D., GAMMINO, S. & ANDO, L. (2007). Ion energy increase in laser-generated plasma expanding through axial magnetic field trap. *Laser Part. Beams* **25**, 453–464.

TSUI, Y.Y., MINAMI, H., VICK, D. & FEDOSEJEVS, R.J. (2002). Debris reduction for copper and diamond-like carbon thin films produced by magnetically guided pulsed laser deposition *J. Vac. Sci. Technol. A* **20**, 744.

VEIKO, V.P., SHAKHNO, E.A., SMIRNOV, V.N., MIASKOVSKI, A.M. & NIKISHIN, G.D. (2006). Laser-induced film deposition by LIFT: Physical mechanisms and applications. *Laser Part. Beams* **24**, 203–209.

RAI, V.N., SINGH, J.P., YUEH, F.Y. & COOK, R. (2003). Study of optical emission from laser-produced plasma expanding across an external magnetic field. *Laser Part. Beams* **21**, 65.

WAGNER, A.J., CARLO, S.R., CHAD, V. & FAIRBROTHER, D.H. (2002). Effect of X-ray radiation on the chemical and physical properties of a semifluorinated self assembled monolayer. *Langmuir* **18**, 1542.

WANG, Y.L., XU, W., ZHOU, Y., CHU, L.Z. & FU, G.S. (2007). Influence of pulse repetition rate on the average size of silicon nanoparticles deposited by laser ablation. *Laser Part. Beams* **25**, 9–13.

WIEGER, V., STRASSL, M. & WINTNER, E. (2006). Pico- and microsecond laser ablation of dental restorative materials. *Laser Part. Beams* **24**, 41–45.

WOLOWSKI, J., BADZIAK, J., CZARNECKA, A., PARYS, P., PISAREK, M., ROSINSKI, M., TURAN, R. & YERCI, S. (2007). Application of pulsed laser deposition and laser-induced ion implantation for formation of semiconductor nano-crystallites. *Laser Part. Beams* **25**, 65–69.